

The Role of Preconditioning on Morphology Development in Layered Silicate Thermoset Nanocomposites

Tia Benson Tolle,¹ David P. Anderson²

¹Air Force Research Laboratory, Materials and Manufacturing Directorate, Wright-Patterson Air Force Base, Ohio 45433-7750

²University of Dayton Research Institute, 300 College Park, Dayton, Ohio 45469-0168

Received 15 December 2002; accepted 28 May 2003

ABSTRACT: The impact of preconditioning constituent materials on the morphology development of organically modified montmorillonite–epoxy nanocomposites is examined to determine the sensitivity of exfoliation to material conditions. *In situ* synchrotron small-angle X-ray scattering studies were performed to relate the initiation and levels of exfoliated morphologies with various silicate preconditioning processes. Significantly, exfoliation could be achieved in systems initially considered intercalated by preconditioning

through epoxy–silicate mixture aging. The resulting morphologies lead to slightly improved toughness. Implications for nanocomposite morphology development models include the necessity of further investigation of the complexities of both local and global morphologies. © 2003 Wiley Periodicals, Inc. *J Appl Polym Sci* 91: 89–100, 2004

Key words: nanocomposite; epoxy; layered silicate; morphology; processing

INTRODUCTION

Polymeric nanocomposites offer opportunities to explore new and enhanced material properties beyond what is currently available in polymeric composites. Many combinations of nanoscale constituents and polymeric matrices have been studied over the past decade and significant effects on mechanical, thermal, and physical properties have been observed.^{1,2} Unique to nanocomposites is the achievement of such effects through incorporation of nanoconstituents at weight fractions on the order of only 3 to 5%. Whereas fillers such as silica have historically been incorporated within epoxy resins to modify cure shrinkage, water absorption, and thermal properties and to reduce cost, weight fractions as high as 20 to 50% were required to achieve the desired effects.^{3,4} The potential for new or significantly improved properties attainable at such low-volume fractions is the primary motivation for investigating polymeric nanocomposites for aerospace applications. This attribute enables the incorporation of nanoscale constituents into composite matrices for increased tailoring and new or modified properties without significantly altering the original property suite or existing processing techniques. Crucial to the ability to investigate such benefits is the development

of in-depth understandings of morphologies and their evolution.

A large portion of polymeric nanocomposite research utilizes the mineral montmorillonite (MMT), a 2 : 1 layered silicate composed of repeating unit layers of two silica tetrahedral sheets fused to an edge-shared central alumina octahedral sheet. In the space between a plane in a given unit layer and the corresponding plane in the next unit layer, defined as the gallery, oxygen layers of neighboring units are adjacent to each other, resulting in weak van der Waals bonds. Though in its natural state the layers are hydrophilic and incompatible with hydrophobic organic polymers, modifications through cation-exchange reactions can render the layers organophilic.^{5,6} Polymer intercalation is enabled in this environment, and two idealized morphologies are often described⁷: (1) intercalated morphologies, which occur when a single or few polymer chains enter the gallery of the silicate and the basal planes expand (typically on the order of 10 to 40 Å), retaining their stack-like registry and association; and (2) exfoliated morphologies, which result when the layers are highly separated (typically on the order of 100 Å or more) and are well dispersed and usually disordered within the polymer. However, it is more common that layered silicate nanocomposites exhibit variations and combinations of these idealized morphologies such that morphology descriptions must not only take into account layer-to-layer associations (*d*-spacing) but also higher scale orders.^{8–10} Thus, enhanced understanding of morphology development is hampered by the challenge of adequate morphology characterization and description.

Correspondence to: T. B. Tolle (tia.bensontolle@wpafb.af.mil).

Contract grant sponsor: U.S. Air Force; contract grant number: F33615-00-D-5006.

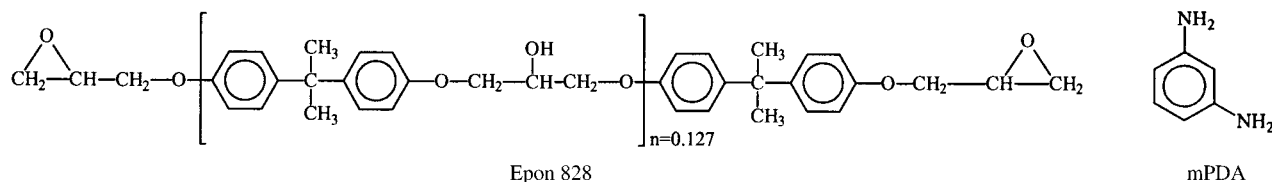


Figure 1 Chemical structures of Epon 828 epoxy and cure agent *m*-phenylenediamine (mPDA).

Although many thermoplastic nanocomposites have been investigated since the pioneering achievements of the Toyota group in the late 1980s, only recently has research addressed epoxy nanocomposite morphology descriptions and models so critical in the development of process–morphology correlations and controlled systems.^{11–14} One of the specific challenges associated with describing epoxy nanocomposite morphology development is quantifying the role played by the numerous processing variables that affect network development and thus morphology formation. These variables include time, temperature, and other process history such as shear.^{15,16} In addition to processing variables, many constituent variations are known to play a role in layered silicate nanocomposite morphology such as charge density of the silicate surface, compatibility between the silicate and the polymer, the nature of the polymer (polar or apolar), and chain length and structure of the cationic surfactant/modification.^{6,17–22} Also, the organic modifications of MMTs affect the initial size of the gallery and may participate in the polymerization process.^{6,20,23–25} Such numerous variables suggest that morphology development in layered silicate epoxy nanocomposites is quite complex. To date, the understanding of its complexity, as evidenced by the literature, and the effect of various processing and material variables are limited.

A fundamental understanding of the morphology development events can provide researchers with the insight needed to control nanocomposite morphologies, hence, morphology-sensitive properties and manufacturing processes. The many scales at which nanocomposite morphologies occur makes this a challenging endeavor. The galleries themselves, so important to morphology development, may also contain complex gradients of physical and chemical properties from silicate layer to silicate layer. This complexity must ultimately be recognized for control of processing, morphologies, properties, and model development. In this work, effects of material preparation variation on morphology development are explored. Although the results reported here generally agree with those others have observed in morphology development of epoxy nanocomposites, through *in situ* small-angle X-ray scattering (SAXS), transmission electron microscopy (TEM), and thermal characterization, subtle inconsistencies are found that emphasize

the crucial need for further characterization of morphologies at all scales.

EXPERIMENTAL

Materials

Two organically modified layered silicates (OLS) with similar chemical modifications but different cation exchange capacities (CEC) and fabrication techniques were utilized: I.30E, a commercially available product from Nanacor (Arlington Heights, IL) (CEC ~ 145 meq/100 g based on octadecylammonium-treated MMT), and SC18, a similar organoclay prepared in the laboratory (CEC ~ 92 meq/100 g).²⁶ Epon 828 epoxy [Shell Chemical Co., Houston, TX; low molecular weight diglycidyl ether of bisphenol A (DGEBA)] was cured with *m*-phenylenediamine (mPDA; Sigma-Aldrich Chemical Co., St. Louis, MO), an aromatic amine-based cure agent, at a stoichiometric ratio to provide glassy thermosetting systems (Fig. 1).

The nanocomposites were prepared by *in situ* intercalative polymerization. The epoxy was heated to 60°C and OLS in the amount to achieve a final fraction of 5% by weight was added directly to the epoxy. The silicate–epoxy mixture was mixed with a magnetic stir bar for 1 h while maintaining the temperature at 60°C. In the baseline process, the mixture was degassed under vacuum at 60°C; the cure agent was melted (in the range of 60 to 65°C), and then the appropriate amount of cure agent was mixed well with the epoxy silicate mixture at 60 to 65°C. Preconditioning by aging the silicate–epoxy mixture was performed and composed of variations in the elapsed time between preparation of the silicate–epoxy mixture and the addition of the cure agent. This process, here called “mixture aging,” was achieved at room temperature for periods ranging from a few hours to a number of weeks.

Characterization

For SAXS studies, the epoxy–silicate–cure agent mixture was placed in a copper sample holder with Kapton tape windows in a programmable oven cell within the X-ray beam. The thickness of the sample thus formed was approximately 2 mm. Measurements

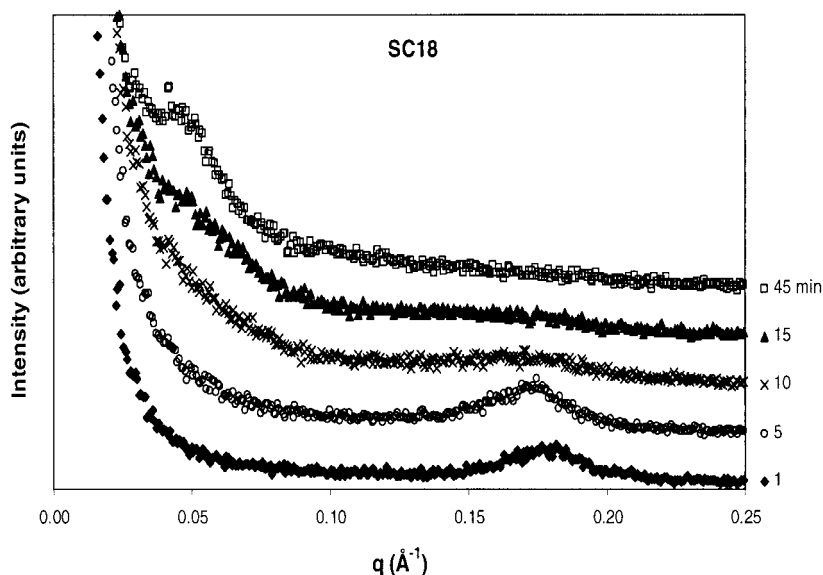


Figure 2 Time-dependent small-angle X-ray scattering data for SC18/Epon 828/mPDA at isothermal temperature of 80°C (intensity data offset for clarity).

were conducted at the National Synchrotron Light Source at Brookhaven National Laboratory on Beamline X27C utilizing a 1-D detector ($\lambda = 0.1366$ nm). Scattering data, intensity (I) versus detector position, were collected and stored for subsequent analysis. The scattering momentum transfer vector q was calculated from the calibrated detector position and is defined as $q = (4\pi/\lambda)\sin \theta$, where θ is half the scattering angle and λ is the wavelength of the incident beam. All SAXS experiments were conducted at an isothermal temperature of 80°C. Scattering data were corrected for background and fitted through the use of PeakFit™ curve fitting software.

Thermal data were obtained on a Thermal Instruments differential scanning calorimeter 2820 at 10°C/min under nitrogen. Transmission electron micrographs were obtained on cryomicrotomed samples to minimize deformation-induced morphologies by using a Reichert–Jung ultracut microtome equipped with a 45° diamond knife and mounted on 200-mesh copper grids. Bright field images were obtained on a Phillips CM200 transmission electron microscope with a LaB₆ filament operating at 200 kV. Fracture toughness was calculated from compact tension specimens per ASTM standard E399. Statistical data were generated from three loadings per sample, 10 samples per material. Dynamic mechanical analysis was performed by using a Rheometrics Ares dynamic spectrometer at a frequency of 100 rad/s, heating rate of 2°C/min, and strain of 0.1%.

RESULTS AND DISCUSSION

SAXS studies are uniquely suited to capturing averaged information about both intercalated and exfoli-

ated states and, in the case of synchrotron sources, to study real-time nanoscale morphology development. TEM complements such studies with specific local morphology information. Neither method alone provides information on a sufficient volume of material from which to draw overall morphology conclusions, especially in light of the multiple combinations and scales on which morphologies can occur. Therefore, their combined use is critical. Thermal characterization can also provide information on variables that influence exfoliation, specifically, the potential role of network formation.

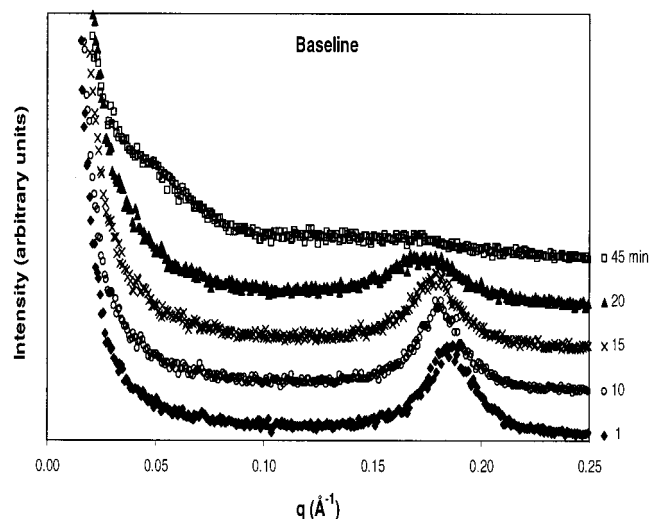


Figure 3 Time-dependent small-angle X-ray scattering data for baseline (no aging) I.30E/Epon 828/mPDA at isothermal temperature of 80°C (intensity data offset for clarity).

TABLE I
The d -Spacings Reached by I.30E/Epon 828/mPDA at an Isothermal Temperature of 80°C Showing the Effects of Mixture Aging

Weight fraction I.30E	Fabrication process	Initial d -spacing (Å)	d -spacing at 60 min (Å)
5%	Baseline	34	42 ^a
5%	Epoxy-silicate mixture aged 1 week	34	45
5%	Epoxy-silicate mixture aged 4+ weeks	36	104
5%	Epoxy-silicate mixture aged 8 weeks	35	105
5%	Epoxy-silicate mixture aged 16+ weeks	36	110
7%	Baseline	33	37
7%	Epoxy-silicate mixture aged 16+ weeks	35	106

^a Final time: 45 min Error typically within 1 Å.

Information on the development of layered silicate nanocomposite morphology can be obtained from analysis of small-angle scattering data, ranging from the absence or presence of a Bragg peak; the evolution of the peak position with material composition and processing conditions; the breadth of the peak (which relates to degree of order); and power law decay at low q for large-scale organization information. Both silicate systems were effectively intercalated with the epoxy resin upon mixing, with average d -spacings on the order of 35 Å. As can be seen in Figures 2 and 3, behavior at temperature with the addition of the cure agent is representative of what is typically observed for epoxy-based nanocomposites, with initial Bragg peaks that shift to marginally lower q and broaden with time and then disappear, and finally the subsequently the appearance and development of a low q peak occurs.^{13,25}

Surfactant density

At 80°C for 45 min, the SC18 silicate-based material reached basal spacings of over 100 Å from initial spacings of 36 Å; the I.30E-based material reached spacings of just over 40 Å from initial spacings of 34 Å. In general, differences in d -spacing development with time between the I.30E- and SC18-based nanocomposites may be partially explained by the number density of surfactant chains and intergallery order. These two OLSs differ in that the SC18 OLS fabrication process is well controlled and completely washes out excess surfactant, which is not the case for the I.30E material.^{26,27} These two silicates also represent opposite extremes of CEC typically exhibited by natural montmorillonite minerals, which range from 80 to 150 meq/100 g.²⁰ As intergallery packing density of the intercalated organic modifications parallels the CEC of the host silicate, the higher number of surfactant chains will result in a smaller relative fraction of intergallery epoxy. As expected, initial silicate basal spacing is larger for the higher exchange capacity system, I.30E. Order and orientation of these organic modifier chains, affected by their confinement within the silicate layers, are

higher with higher intergallery packing density, as shown by Vaia.²⁸ Such different amounts of surfactant and states of order promote different levels of mobility of the intergallery chains, which may affect the manner in which the epoxy and, subsequently, the cure agent intercalates the galleries of the OLS, thus biasing the balance between intra- and extragallery network formation toward the latter. This would result in less expanded layers as observed here. The greater amount of surfactant within the I.30E system (and lesser relative fraction of epoxy) provides for different reactant ratios and may also accelerate network formation, impeding exfoliation as compared to the SC18 system. These differences in morphology due to subtle variations in similar constituents reinforce the importance of material and process history and variations in investigations of nanocomposite morphology. For the remainder of the study reported here, a single OLS constituent—I.30E—was utilized and material preparation process varied.

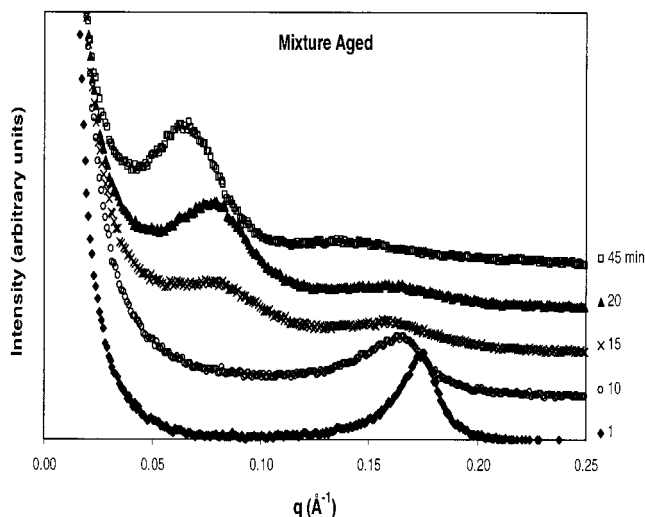


Figure 4 Time-dependent small-angle X-ray scattering data for I.30E/Epon 828/mPDA at isothermal temperature of 80°C after mixture aging for 16 weeks (intensity data offset for clarity).

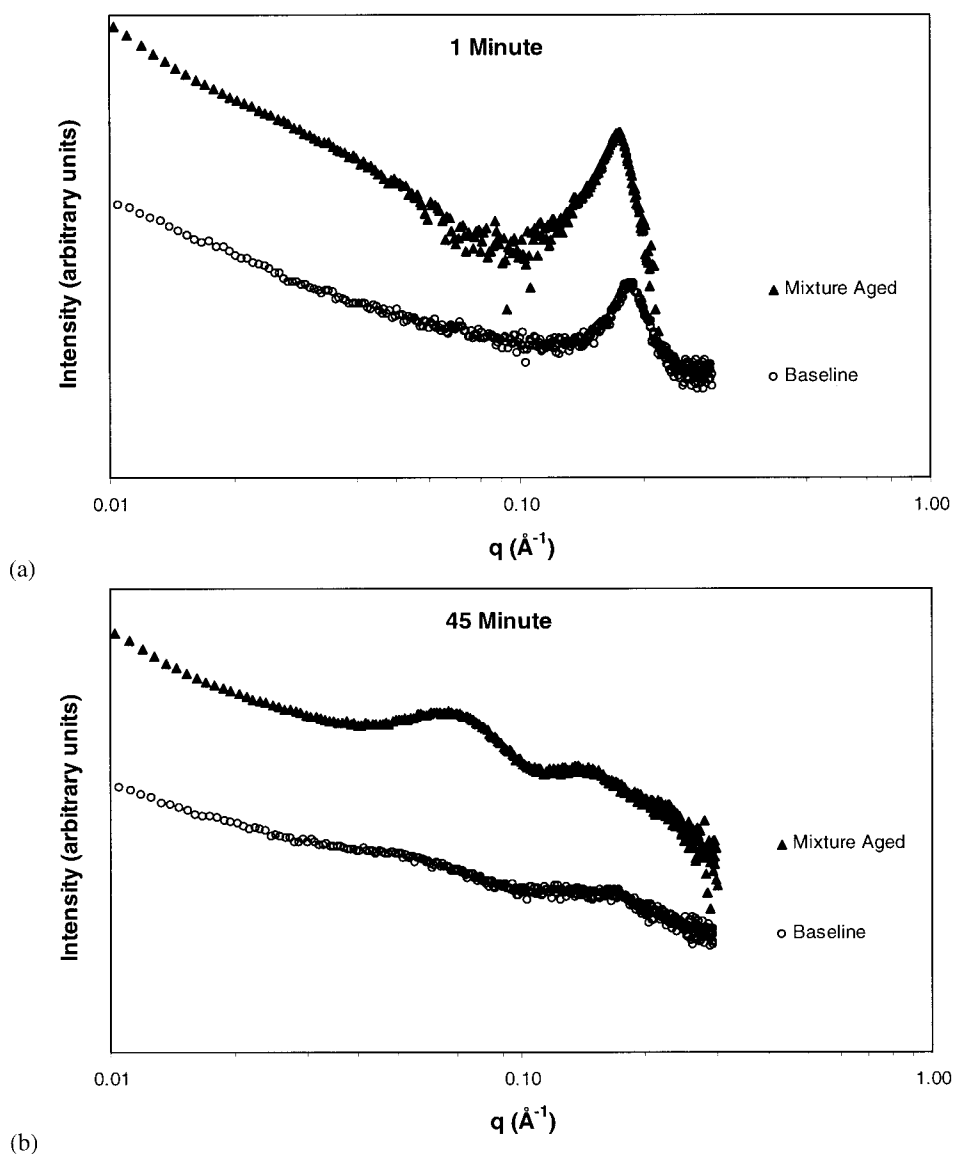


Figure 5 Small-angle X-ray data for baseline material (a) and mixture-aged materials (b) show similar behavior initially (1 min) but differ significantly in the low q region slope and Bragg peaks after 45 min at 80°C.

Mixture aging preconditioning

Variations on the age of the I.30E epoxy mixtures were explored and resulted in dramatically different exfoliation development behaviors (Table I). Scattering data on materials that had undergone long-term mixture aging prior to addition of cure agent exhibited distinctly different features related to morphology as compared with samples that underwent the baseline fabrication process. Figure 4 shows scattering curves from materials which had been mixture aged for 16 weeks; significant differences in scattering can be seen in comparison to the baseline material shown in Figure 3. Mixture-aged samples exhibited initiation of gallery expansion in significantly shorter times as evidenced by the loss of the peak associated with the initial intercalated morphology. With isothermal heat-

ing at 80°C, peak intensity associated with intercalation ($q \sim 0.18 \text{ \AA}^{-1}$, d -spacing $\sim 35 \text{ \AA}$) for the material that underwent the longest mixture-aging time reached half of its initial intensity within 10 min as compared to 20 min for baseline samples. Peak breadth, an indication of the size of the scatterer domains, was narrower for the mixture-aged materials, implying a longer range persistence of the dominant scattering morphology and less disorder. Most significant was the difference in scattering in the range of $q < 0.1 \text{ \AA}^{-1}$, or structures $> 100 \text{ \AA}$, with mixture-aged samples exhibiting a clear and gradual development of a Bragg peak within 45 min at 80°C. Note that the baseline material did not clearly develop such peaks within this time period. The manner in which such a peak develops with time differs from that of the base-

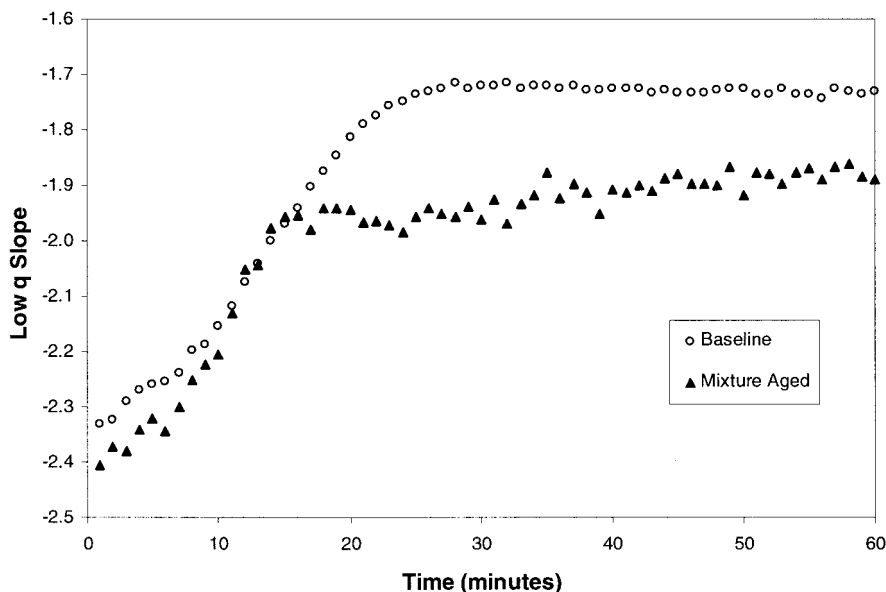


Figure 6 Low q slopes for materials versus time show earlier onset of slope stabilization for mixture-aged materials.

line as well. In previous studies of epoxy nanocomposites both here and elsewhere, trends on the loss of peaks associated with intercalated morphology and the development of peaks associated with exfoliated morphology have been observed to occur as if through a rapid transition, with pertinent peaks appearing to be mutually exclusive.^{25,26} Such observations suggest a rapid loss of intercalated morphology and subsequent development of exfoliated morphology. The lack of clear Bragg peaks during this period may be due to a loss of initial registry and order through network formation. Extragallery network formation may occur closely thereafter and limit mobility before the layers are fully expanded and reach more ordered states. This would provide a model in which minimal low q peak development occurs prior to gelation. The development of Bragg peaks associated with exfoliated morphology in mixture-aged materials occurs simultaneously with the loss of peaks associated with intercalated morphology. Two distinct and ordered morphologies coexisted during the process, which is clearly seen in Figure 4.

Understanding the role that the balance between intragallery and extragallery network formation plays on exfoliation in layered silicate epoxy nanocomposites has increased over the past several years.^{11,12,29} Intragallery network formation, extragallery network formation, and diffusion of resin and cure agents are all key variables in the formation of exfoliated morphologies. The findings and potential explanations from this research are consistent with the model proposed by Lan et al., in which intragallery crosslinking rates must be higher than extragallery rates to allow for the development of exfoliation.¹¹ Normal extragallery network formation would be expected for the

materials studied here upon addition of the cure agent, with the primary differences being acceleration effects and network formation within proximity of the silicates. Chin et al. observed exfoliation with the same materials studied in this work only under suppression of extragallery crosslinking through the use of less than stoichiometric amounts of cure agent and elevated temperatures.¹³ The systems studied here provided a well-ordered development of structure similar to that reported by Chin with no cure agent at high temperature, with the exception of the manner in which the peaks developed. Normal extragallery network formation would be expected for the materials studied here upon addition of the cure agent, with primary differences being acceleration effects and network formation within proximity of the silicates. The different behaviors observed here suggest that the role of the zone within close proximity of the silicate is important to morphology development as is the recognition of the nonhomogeneity of intragallery and interfacial regions.

A characteristic feature of scattering from disordered and fractal systems is a power law relationship; in regions where $qa \gg 1$, where a is a characteristic length of the scatterer, $I(q) \sim q^{-\alpha}$.^{30,31} For well-defined, simple geometric particles, it has been shown that α reflects the dimensionality of the object (four for three-dimensional objects such as spheres; two for quasi-two-dimensional bodies such as disks of negligible thickness; and one for quasi-one-dimensional elements such as thin rods). More complex structures, or "mass fractals," can be similarly characterized but with nonintegral exponents. Differences in the low q power law behavior, an indicator of more global structure and morphology at a scale on the order of hun-

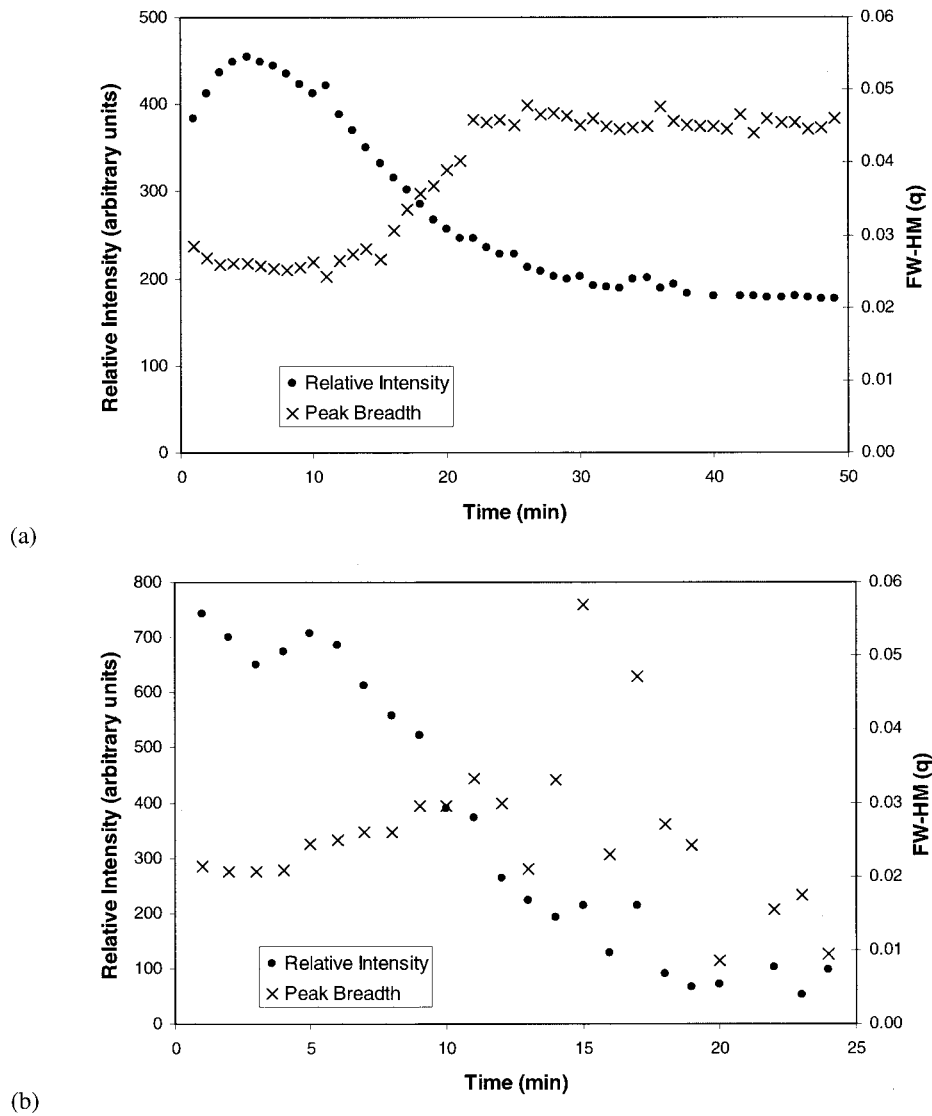


Figure 7 Time for loss of scattering intensity of initial Bragg peak [~ 28 min for baseline (a), ~ 17 min for mixture aged (b)] corresponds with onset of stabilization of low q slopes. (Difficulty in fitting peak breadth causing scatter in data.)

dreds of \AA , are observed between baseline and mixture-aged materials (Fig. 5). Both baseline and mixture-aged materials follow $I(q) \sim q^{-2.5}$ initially, then tend toward $I(q) \sim q^{-1.9}$, with time at 80°C . These power law behaviors show a trend toward sparser structures if a mass fractal interpretation is used.³² The various power law slope regions, indicative of morphologies, as well as the breaks in the slopes, indicative of length scales, also differ. The low q slope trend with time, depicted in Figure 6, shows a strong dependence upon the mixture-aging condition of the materials. The time at which the slope undergoes a significant transition occurs sooner for the material that underwent the longest aging, at approximately 16 as compared to 23 min. Once past the knee in the curve, the slope continues to increase slightly with time for

the aged materials, whereas the slope for the baseline materials appears to stabilize. The slope trend goes toward more two-dimensional scatterers for the mixture-aged material, possibly indicative of tactoid development through gallery expansion. The knees in the curve correspond well with the minimum intensity of Bragg scattering from the initial intercalated structures of 34\AA d -spacings (Fig. 7). At this point, the initial well-ordered intercalated morphology no longer dominates the material.

The significant differences in morphology states between these two conditions are depicted clearly in TEM images (Fig. 8). Although it is possible to distinguish multiple as well as hierarchies of morphologies within a single TEM image, analysis of multiple images reveals a dominant morphology in the baseline

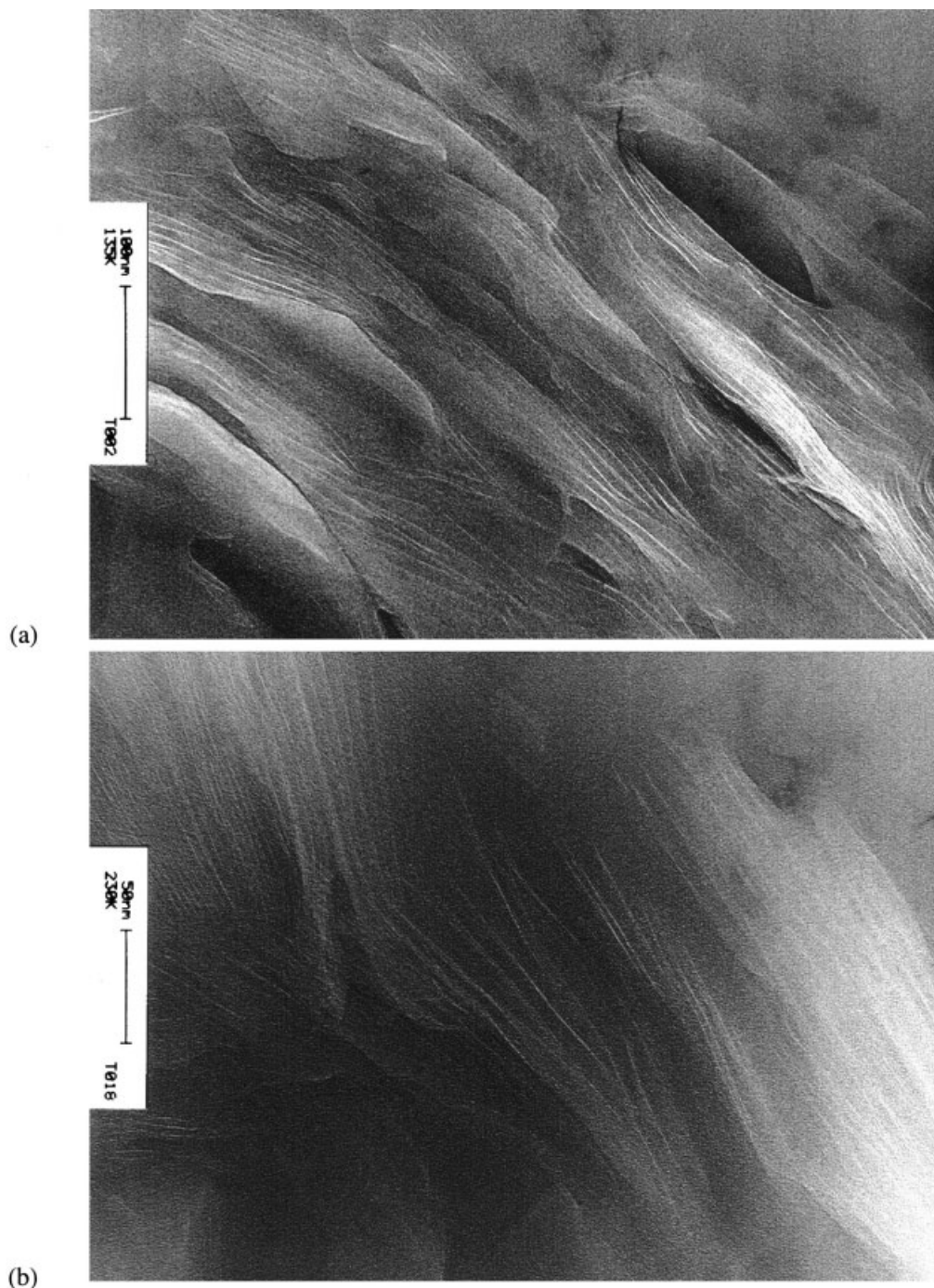


Figure 8 TEM images of unaged [(a) and (b)] and aged [(c) and (d)] I.30E/Epon 828/mPDA nanocomposites.

materials that are intercalated, with straight OLS layers separated typically by constant spacings of 25 to 75 Å and associated in tactoids of five to nine layers. On a higher scale, tactoids are generally parallel to each other or at small angles and are separated by 50 to 150 Å. The dominant morphology for the materials that underwent mixture aging included much less ordered tactoids, many in packs of four OLS layers with spacings of approximately 80 Å. Tactoids are generally parallel, separated by 75 Å through over 600 Å. Some

tactoids also exhibited gradient spacings in which layers were separated by increasing distances through a tactoid. For both material systems, multiple levels and mixtures of intercalated and exfoliated morphologies can be found (as well as some silicates that are not intercalated). In general, mixture-aging results in a more expanded or ordered exfoliated morphology state with smaller colonies of tactoids; the baseline material shows an ordered intercalated morphology with longer range registry both within and between tactoids.

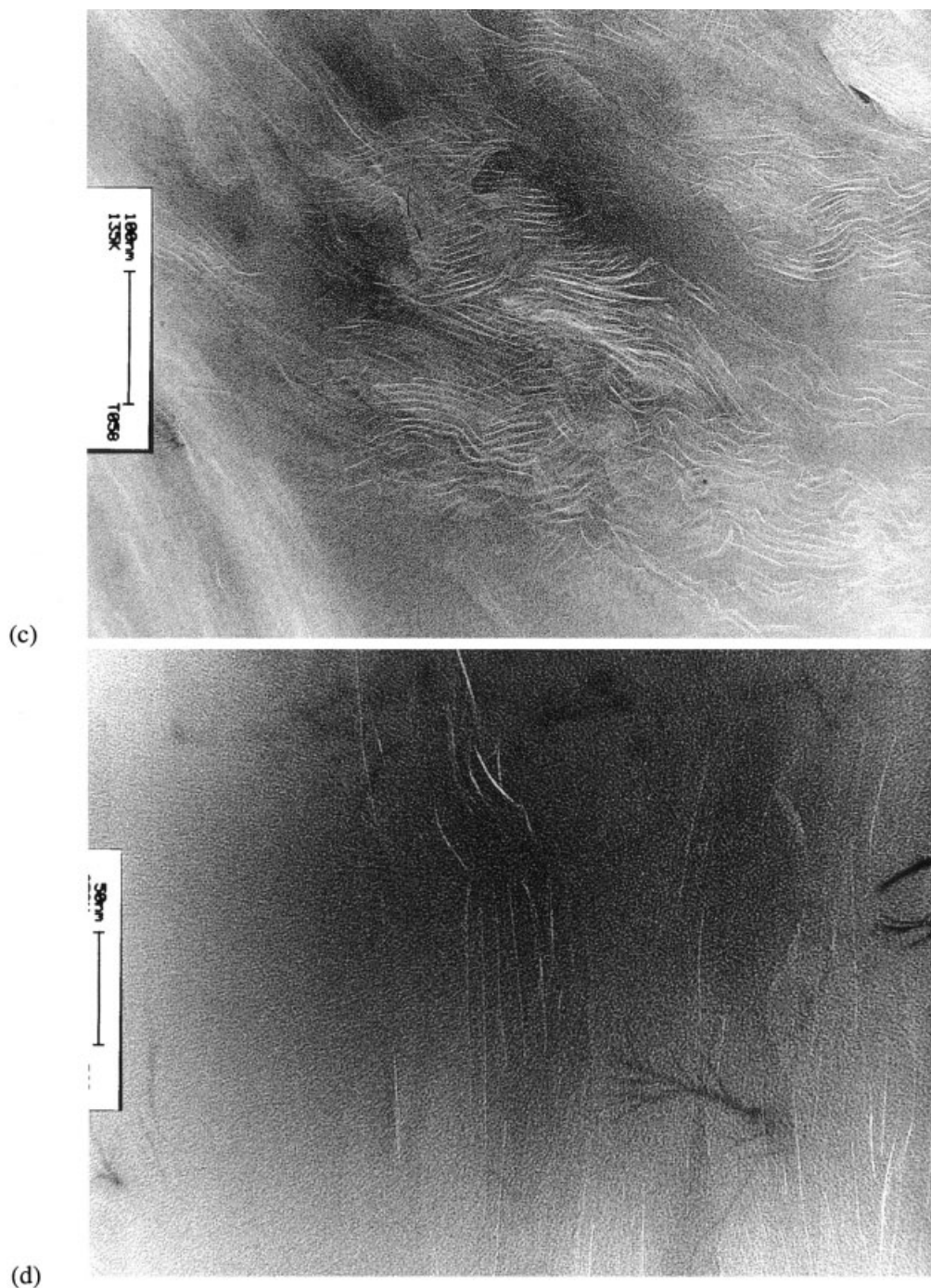


Figure 8 (Continued from previous page)

The network formation process appears to be of great importance in morphology development in nanocomposites. Differential scanning calorimetry (DSC) data show that the addition of I.30E results in a significantly earlier onset of polymerization as compared with that for the epoxy-cure agent alone (Table II). This reaction acceleration behavior has been observed in other epoxy systems.^{21,33,34} DSC analysis of the epoxy and I.30E without the primary cure agent shows that the silicate accelerates the epoxy homo-

polymerization reaction as well; however, homopolymerization with or without I.30E occurred at temperatures much higher than those studied in the scattering experiments; thus, early reaction onset is not believed to be a homopolymerization reaction (data not shown). As has been observed by others, DSC, similar to the TEM and scattering data, recognizes the complexity of morphology, with a slight exotherm after the main cure exotherm observable in some of the systems which may be due to nonuniform network

TABLE II
DSC Data for Preconditioned I.30E/Epon 282/mPDA Materials

Material	T_{onset} (°C)	T_{max} (°C)	ΔH_{rxn} (cal/g) (normalized to epoxy content)
Epon 828/mPDA	126	158	106
I.30E/Epon 828/mPDA baseline	84	130	103
I.30E/Epon 828/mPDA aged 2 day	85	136	99
I.30E/Epon 828/mPDA aged 1 week	87	136	101
I.30E/Epon 828/mPDA aged 8 weeks	93	141	76
I.30E/Epon 828/mPDA aged 16 weeks	107	154	96

formation.³⁵ Preconditioning through mixture aging minimizes the advancement of reaction onset (Table II). It is likely that the mixture-aged materials studied here underwent some epoxy reaction over the mixture-aging time such that the ability of the organically modified silicate to accelerate the epoxy-amine reaction is reduced.³⁶ If so, final network formation for these materials may have occurred under slightly excess cure agent. Here, the effects of the OLS on network formation and ultimate network density must be accounted for not only within the morphology of the OLS constituent but also for the polymer itself. The DSC data coupled with the SAXS and TEM observations suggests that accelerated network formation due to the OLS hinders tactoid expansion.

In addition to differences in the amounts of various reactants due to mixture aging, differences in the types of reactants may play a role in the development of exfoliated morphology. In reactions of epoxy with aromatic amines, network development occurs through the initial formation of linear polymer molecules of high molecular weight, which then crosslink to form a network, with some remaining uncrosslinked. In contrast, with aliphatic amines network development initiates with the formation of branched, low molecular weight polymer molecules, which then link to form a highly crosslinked network.¹⁵ In baseline samples, network formation within close proximity to the silicate surface, here termed “the interphase region,” may be primarily driven by the aromatic amine cure agent reacting with the epoxy-silicate mixture, with the interfacial region of the organically modified silicate able to participate in network formation. Acceleration of this reaction by the hydroxyls on the edges of the silicate may cause rapid network formation within and around the tactoids, effectively limiting mobility of individual layers and freezing intercalated morphologies. As seen in Figure 3, gallery expansion of the mixture-aged materials continues to develop well beyond 30 min at 80°C. Slight network formation in the interphase region of the mixture-aged materials may form over the mixture-aging time through reaction with hydroxyl groups, the ammonium, and any aliphatic amines and may provide a less reactive interfacial region. Partici-

pation in the subsequent cure-agent induced network formation would thus be minimized, and the balance between network formation within and around the tactoids would be favorable to OLS mobility prior to gelation. These subtle variations in the interface and interphase regions may alter the balance of intra- and extragallery network formation to cause the differences observed here in morphology development. The differences observed through SAXS, DSC, and TEM due to the material preconditioning studied here could be significant factors in an observation or phenomenological-based model of morphology and exfoliation development and offer motivation for the recognition of unexpected complexities in layered silicate thermoset nanocomposites because of material and process variations.

Mechanical properties

The potential of nanomodifications to achieve an improved toughness-stiffness balance is the instigation of much research,^{37,38} yet general trends have not been conclusively demonstrated for the effects of nanomodifications on toughness. Of the many existing variables that can affect energy dissipation mechanisms and apparent toughness results, morphologies on various scales are of well-known importance. Historically, thermosetting resins such as epoxies have key engineering limitations including inherent brittleness and moisture uptake. Plane strain fracture toughness results for the nanocomposites exhibit higher toughness than the epoxy alone. Toughness results are seen to differ between the baseline and mixture-aged materials, with the mixture-aged material marginally tougher than the baseline material (Table III). Here, both the various polymer network and nanocomposite morphologies may play roles in the toughness data and suggest that in some cases material conditioning may be a strong factor in morphology-sensitive properties. Dynamic mechanical analysis (DMA) shows that the storage and loss moduli of the nanocomposites are slightly higher than that of the neat resin in the glassy state, with the mixture-aged material marginally higher. The storage modulus improvement is more extreme in the rubber state than in the glassy

TABLE III
Fracture Toughness of I.30E/Epon 828/mPDA Materials

Material	K_{Ic} (psi in ^{0.5})
Epon 828/mPDA (no OLS)	646 ± 270
I.30E/Epon 828/mPDA baseline	913 ± 148
I.30E/Epon 828/mPDA aged 4 mo	1121 ± 343

Note. Data from three loadings per sample, 10 samples per material with the exception of Epon 828/mPDA (no OLS), in which case data are additionally on two batches of material.

state, as has been observed in most layered silicate thermoset nanocomposites. The glass transition temperature based on the $\tan \delta$ ($\tan \delta$ defined as G''/G') was higher for the nanocomposites compared with the epoxy, but approximately the same for the two nanocomposites. The glass transition temperature as defined by G' was slightly higher for the mixture-aged nanocomposite (Fig. 9).

Conclusion

In situ observation of morphology development in layered silicate thermoset nanocomposites offers the opportunity to gain insights necessary for modeling the development of morphology with processing and, ultimately, with correlations of morphology with properties, enabling the design of nanocomposites toward specific desired behaviors. Aging of the silicate-epoxy mixture dramatically changed the development of morphology, resulting in more expanded or ordered exfoliated systems with high

fracture toughness. Interaction between the OLS and the epoxy prior to polymerization may therefore play a large role in how morphology and, specifically, exfoliation develops. Though the complete effects on properties for cured nanocomposites are not readily apparent at this point, the recognition of the complexity, nonhomogeneity, and condition of the material within the galleries must be accounted for to achieve material control and development. Chemistry and structure gradients and regions within the galleries exist and may be found to add complexities to processing and ultimate process control. The diverse behaviors observed here reveal the very complex nature of morphology development in layered silicate epoxy nanocomposites and the need for future efforts toward its understanding and complete characterization. Processing or material variables such as the mixture aging explored here may be found to play a dominant role in the ability of a given material system's ability to reach exfoliated morphologies. A higher degree of material control may be required until we can better characterize, understand, and predict nanocomposite morphology development.

The authors acknowledge the guidance and encouragement provided by Dr. Nicholas J. Pagano throughout this research and associated manuscript preparation and the insightful and valuable technical discussions with Dr. Richard A. Vaia. The authors also thank Dr. Kahlid Lafdi for TEMs and Dr. Chenggang Chen for supplying the SC18 silicate materials. The use of the National Synchrotron Light Source at Brookhaven National Laboratory, without which this work

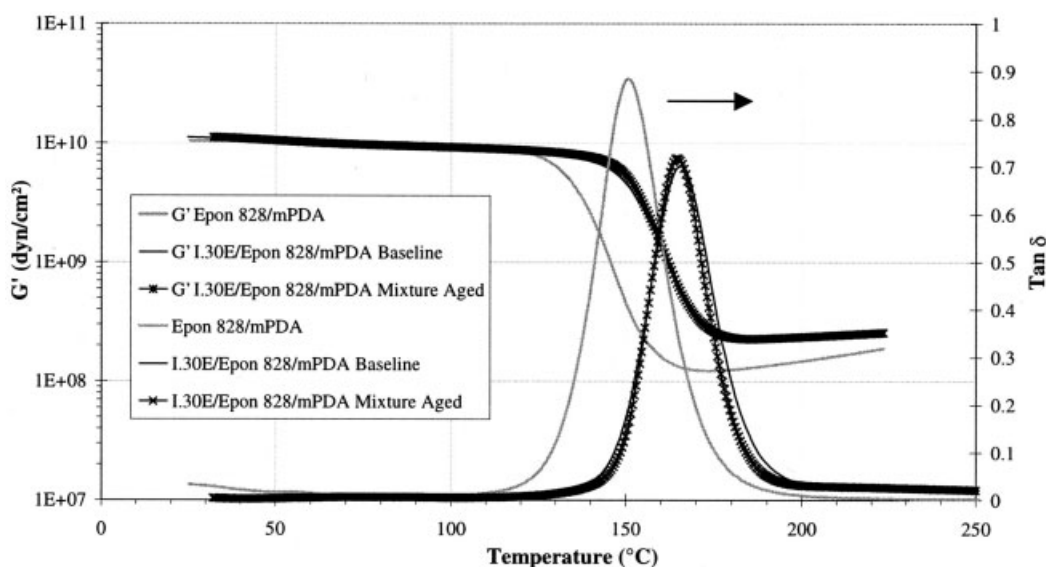


Figure 9 Storage modulus and $\tan \delta$ curve for Epon 828/mPDA (no OLS), I.30E/Epon 828/mPDA baseline process, and I.30E/Epon 828/mPDA mixture aged.

would not have been possible, is also gratefully acknowledged, as is the U.S. Air Force for partial support of this research via Contract F33615-00-D-5006.

References

1. Alexandre, M.; Dubois, P. *Mater Sci Eng* 2000, 28, 1.
2. Pinnavaia, T. J.; Beall, G. W. *Polymer-Clay Nanocomposites*; Wiley: Chichester, 2000.
3. Deanin, R. D.; Schott, N. R. *Fillers and Reinforcements for Plastics*; American Chemical Society: Washington, DC, 1974.
4. Neilsen, L. E. *Mechanical Properties of Polymers and Composites*; Marcel Dekker: New York, 1994.
5. Moore, D.; Reynolds, R. *X-ray Diffraction and the Identification and Analysis of Clay Minerals*; Oxford Univ. Press: New York, 1997.
6. Theng, B. K. *The Chemistry of Clay-Organic Reactions*; Wiley: New York, 1974.
7. Vaia, R. A.; Giannelis, E. P. *Macromolecules* 1997, 30, 7990, 8000.
8. Morgan, A. B.; Gilman, J. W.; Jackson, C. L. *Macromolecules* 2001, 34, 2735.
9. Bharadway, R. K.; Mehrabi, A. R.; Hamilton, C.; Trujillo, C.; Murga, M.; Fan, R.; Chavira, A.; Thompson, A. K. *Polymer* 2002, 43, 3699.
10. Vaia, R. A.; Liu, W. J. *Polym Sci, Part B: Polym Phys* 2002, 40, 1590.
11. Lan, T.; Kaviratna, P. D.; Pinnavaia, T. J. *Chem Mater* 1995, 7, 2144.
12. Kornmann, X.; Lindberg, H.; Berglund, L. A. *Polymer* 2001, 42, 4493.
13. Chin, I.; Thurn-Albrecht, T.; Kim, H.; Russell, T.; Wang, J. *Polymer* 2001, 42, 59471.
14. Wang, K. H., et al. *Polymer* 2001, 42, 9819.
15. May, C. A. *Epoxy Resins Chemistry and Technology*; Marcel Dekker: New York, 1988.
16. Ullett, J. Ph.D. Thesis, University of Dayton, 1992; Brown, J. Ph.D. Thesis, Virginia Polytechnic Institute and State University, 1994.
17. Dennis, H. R.; Hunter, D. L.; Chang, D.; Kim, S.; White, J. L.; Cho, J. W.; Paul, D. R. *Polymer* 2002, 42, 9513.
18. Wang, M. S.; Pinnavaia, T. J. *Chem Mater* 1994, 6, 468.
19. Butzloff, P., et al. *Polym Eng Sci* 2001, 41, 10, 1794.
20. Grim, R. E. *Clay Mineralogy*; McGraw-Hill: New York, 1953.
21. Kornmann, X.; Lindberg, H.; Berglund, L. A. *Polymer* 2001, 42, 1303.
22. Jiankun, L.; Yucai, K.; Zongneng, Q.; Xiao-su, Y., *J Polym Sci, Part B: Polym Phys* 2001, 39, 115.
23. Brown, J. M.; Curliss, D.; Vaia, R. A. *Chem Mater* 2000, 12, 3376.
24. Lan, T.; Kaviratna, D.; Pinnavaia, T. J. *J Phys Chem Solid* 1996, 57, 1005.
25. Benson Tolle, T. H.; Anderson, D. P. *Compos Sci Technol* 2002, 62, 1033.
26. Chen, C.; Curliss, D. *MRS Symp Proc Series* 2001, 703, 3.
27. Hunter, D., Nanocor, Inc., Personal communication, Sept 2002.
28. Vaia, R. A. *Chem Mater* 1994, 6, 1017.
29. Shi, H.; Lan, T.; Pinnavaia, T. J. *Chem Mater* 1996, 8, 1584.
30. Brumberger, H. *Modern Aspects of Small-Angle Scattering*; Kluwer Academic: Netherlands, 1995.
31. Roe, R. J. *Methods of X-Ray and Neutron Scattering in Polymer Science*; Oxford Univ. Press: New York, 2000.
32. Martin, J. E.; Hurd, A. J. *J Appl Crystallog* 1987, 20, 61.
33. Messersmith, P. B.; Giannelis, E. P. *Chem Mater* 1994, 6, 1719.
34. Wang, J. *Chem Mater* 1998, 20, 1820.
35. Ranade, A.; D'Souza, N. A.; Gnade, B. *Polymer* 2002, 43, 3759.
36. Enns, J. G.; Gillham, J. K. *J Appl Polym Sci* 1983, 28, 2567.
37. Kornmann, X.; Berglund, L.; Sterte, J. *Polym Eng Sci* 1998, 38, 1351.
38. Zilg, C.; Muelhaupt, R.; Finter, J. *Macromol Chem Phys* 1999, 200, 661.